

Theory of coherence effects in photoinduced Auger events: Resonant satellites in metals with filled d bands

S. M. Girvin

Surface Science Division, National Bureau of Standards, Washington, D.C. 20234

David R. Penn

Electron Physics Division, National Bureau of Standards, Washington, D.C. 20234

(Received 10 March 1980)

This paper describes a theory of the Auger effect which treats the entire process of core-level excitation followed by decay of the core hole as a coherent sequence of events. We present an approximate analytic solution to the model recently introduced and solved numerically by Davis and Feldkamp. Their model offers an explanation of the resonance behavior of photoemission satellites in metals with filled d bands. Our analytic results help clarify the physics of the resonant satellite phenomena.

Many core-level spectroscopies which are currently receiving theoretical and experimental attention are concerned with the following general sequence of events: An electron is ejected from a core level in an atom or a solid by an incident particle (usually a photon or an electron) after which the core hole decays producing various final-state products. This process must be treated as a coherent whole because of the possibility of incomplete relaxation of the system prior to the final decay event. The phenomenon of incomplete relaxation in x-ray emission and Auger spectroscopy has been studied by several authors.¹⁻⁶ These studies have all been restricted to the case in which the core electron is ejected with very high kinetic energy. It is interesting to consider the alternative situation in which the initial excitation energy is near threshold since the Auger (or x-ray-emission) spectrum may be significantly modified due to the presence of one or more spectator electrons which are a by-product of the process which created the core hole. Davis and Feldkamp⁷ (DF) have recently investigated a model which takes this effect into account. Their numerical calculations exhibit a resonance satellite structure which they attribute to a many-body effect involving the spectator electron. The purpose of this paper is to present an approximate analytic solution to the DF model and to illustrate in detail how coherence between initial creation of the core hole and the Auger decay leads to the satellite structure. As noted by DF, the process is a generalization of the Mahan, Nozières, De Dominicis (MND) x-ray edge problem.⁸⁻¹⁰

We will be concerned with a rather general phenomenon occurring in the Auger spectra of metals in those cases where the spectra are essentially atomic in character. This is the

case for $cc'c''$ spectra; i.e., when an initial core hole c decays via an Auger transition in which it is filled by an electron from core level c' while another electron is excited into the continuum from core level c'' . Another case of interest is the cdd Auger transition in certain metals with filled d bands since in some instances correlation effects can cause the two final-state d holes to remain localized on one atom.¹¹⁻¹⁴ Thus, for example, Cu exhibits an atomic $c-3d-3d$ spectrum while that of Au is bandlike.¹⁵

The DF model was motivated by a number of recent photoemission experiments¹⁶ studying satellite phenomena associated with filled or nearly filled d bands. It has been known¹⁷ for some time that the peak lying 6 eV below the main d -band photoemission peak in Ni is intrinsic, i.e., not associated with energy loss during the escape of the photoelectron. More recently the intensity of the Ni satellite was found to show a large resonance maximum at the photon energy corresponding to the threshold for excitation of an electron from the $3p$ level to the Fermi level.¹⁸ Next came the discovery that in Cu there is a d -band satellite whose relative intensity is considerably weaker than that in Ni.¹⁶ Unlike the Ni case this satellite has significant strength only at photon energies near the $3p$ threshold.

Penn¹⁹ has presented a model to explain the Ni satellite and its associated resonance behavior, but this model is not appropriate to Cu or Zn since it presumes an incompletely filled d band. DF have proposed an entirely new satellite mechanism which should be quite generally operative but dominant only in metals with filled d bands. They propose the following sequence of events. A photon is absorbed creating a $3p$ core hole plus a spectator electron. The core hole then decays leaving two d holes plus a fast Auger electron.

The $3p$ core hole and especially the two d holes which subsequently appear produce a strong perturbation on the conduction electron Fermi sea. This leads to a many-body enhancement of the probability for the spectator electron to end up close to the Fermi level just as in the x-ray edge problem. The result is a satellite peak in the Auger spectrum at constant binding energy (rather than at constant kinetic energy).

The DF model is as follows: Prior to the photoexcitation of a core electron, the conduction electrons obey a free-particle Hamiltonian

$$H_0 = \sum_{k\sigma} \epsilon_k n_{k\sigma}. \quad (1)$$

After core-level photoexcitation the conduction electrons as well as the photoexcited electron experience an attractive contact potential U at the site of the core hole. This introduces a scattering term H_1 into the Hamiltonian

$$H_1 = U \sum_{kk'} c_k^\dagger c_{k'}. \quad (2)$$

The subsequent Auger decay of the core hole leaves the system with two d holes that produce a new potential U' which may be quite strong.

Following DF we ignore the direct photoemission events and consider only the Auger spectrum. Let $R_{\mathbf{x}}(\omega)$ be the rate of production of Auger electrons in state \mathbf{x} with energy $\epsilon_{\mathbf{x}}$ as a function of photon energy ω . Fermi's golden rule gives

$$R_{\mathbf{x}}(\omega) = 2\pi \sum_k f_k |V_{k\mathbf{x}}(\omega)|^2 \delta(\omega - \epsilon_d - \epsilon_{\mathbf{x}} - \epsilon_k), \quad (3)$$

where ϵ_k is the final-state energy of the spectator electron, f_k is the Fermi function, ϵ_d is the energy of the final two- d -hole state, and $V_{k\mathbf{x}}(\omega)$ is the effective matrix element describing the various paths leading to the final state. We begin our analysis with the limiting case $U=0$, $U'<0$. The lowest-order graphs contributing to $V_{k\mathbf{x}}(\omega)$ in this instance are shown in Fig. 1. These are the analogs of the "open-line" diagrams in the x-ray edge problem. There are additional terms corresponding to the "closed loops" in the x-ray edge problem which we ignore for the moment.

The first diagram [Fig. 1(a)] represents

$$V_a = \lambda \frac{1}{\omega - \epsilon_a - \epsilon_k} M, \quad (4)$$

where λ and M are the photon absorption and Auger matrix elements, respectively. For simplicity these are both assumed to be momentum independent. The deep core-hole energy, ϵ_a has the form

$$\epsilon_a = \epsilon_a^0 - i\Gamma, \quad (5)$$

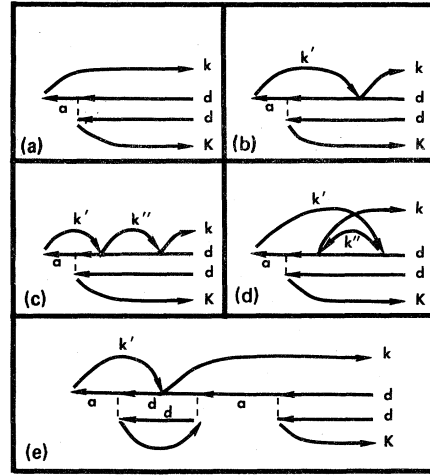


FIG. 1. (a)–(d): Lowest-order diagrams for the Auger spectrum in the case $U=0$, $U' \neq 0$ (electron scattering takes place only after the Auger decay of the core hole). (e): Vertex correction. k , k' , etc., represent the photoexcited electron which scatters from the two-hole d state, K is the Auger electron that is observed in the experiment and "a" represents the core hole.

where 2Γ is the Auger decay rate for the core level. In the absence of any final-state Coulomb interactions, Eq. (4) would represent the only contribution to the effective matrix element. Evaluating Eq. (3) yields

$$R_{\mathbf{x}}^0(\omega) = 2\pi |\lambda M|^2 \frac{1}{(\epsilon_{\mathbf{x}} + \epsilon_d - \epsilon_a^0)^2 + \Gamma^2} \rho(\omega - \epsilon_{\mathbf{x}} - \epsilon_d), \quad (6)$$

where $\rho(\nu)$ is the conduction-band density of empty states.

The other diagrams introduce corrections to the basic Lorentzian Auger line shape of Eq. (6). For example, Fig. 1(b) represents

$$V_b = \lambda \sum_{k'} (1 - f_{k'}) \frac{1}{\omega - \epsilon_a - \epsilon_{k'}} M \frac{1}{\omega - \epsilon_d - \epsilon_{\mathbf{x}} - \epsilon_{k'} + i\delta} U'. \quad (7)$$

Assuming a constant conduction-band density of states ρ , one obtains for the most singular part of V_b

$$V_b \sim V_a \rho U' \{ \ln(-\epsilon_k/\Lambda) - \ln[(\epsilon_a - \omega)/\Lambda] \}, \quad (8)$$

where Λ is a cutoff parameter (assumed to be large) for the potential. Similarly, the diagram in Fig. 1(c) contributes

$$V_c \sim V_b \rho U' \ln(-\epsilon_k/\Lambda), \quad (9)$$

where V_b is given by Eq. (8). Figure 1(d) yields

$$V_d \sim -\frac{1}{2} V_a (\rho U')^2 \{ \ln^2(-\epsilon_k/\Lambda) - \ln^2[(\epsilon_a - \omega)/\Lambda] \}, \quad (10)$$

where the minus sign arises because this is an

exchange diagram. The graph shown in Fig. 1(e) is a typical member of a class of diagrams in which there is a virtual Auger decay which turns on the potential U' and scatters the spectator electron before the system reverts to the original core-hole state. These diagrams all vanish if (as assumed) the core-hole Auger self-energy is frequency independent (i.e., if in the absence of Coulomb interactions the Auger line shape is Lorentzian).

Summing all of the above contributions plus the six third-order diagrams yields

$$V_{k\mathbf{x}}(\omega) = V_a \left[1 + \rho U' \ln \left(\frac{-\epsilon_k}{\epsilon_a - \omega} \right) + \frac{1}{2!} (\rho U')^2 \ln^2 \left(\frac{-\epsilon_k}{\epsilon_a - \omega} \right) + \frac{1}{3!} (\rho U')^3 \ln^3 \left(\frac{-\epsilon_k}{\epsilon_a - \omega} \right) \right], \quad (11)$$

which is the beginning of an exponential series

$$V_{k\mathbf{x}}(\omega) = V_a \exp \left[\rho U' \ln \left(\frac{-\epsilon_k}{\epsilon_a - \omega} \right) \right], \quad (12)$$

similar to the one appearing in the x-ray edge problem [which has $(-\epsilon_k/\Lambda)$ as the argument of the logarithm]. In the x-ray edge problem the Coulomb potential is turned on at the same time that the spectator electron is injected into the conduction band. In the present problem there is a delay between these two events because the Coulomb potential is not turned on until the Auger decay occurs. This accounts for the difference between Eq. (12) and the corresponding x-ray edge amplitude. Equation (12) indicates that many-body effects greatly enhance the transition amplitude when the spectator electron final energy ϵ_k is near zero (the Fermi energy). Since energy must be conserved overall, this results in a satellite peak on the high kinetic-energy side of the Auger line. Another way to understand the appearance of the satellite is from the point of view that the potential U' effectively enhances the density of states near the Fermi energy. Equation (6) then yields two peaks: an Auger peak at $\epsilon_{\mathbf{x}} = \epsilon_a^0 - \epsilon_d$ and a satellite peak at $\epsilon_{\mathbf{x}} = \omega - \epsilon_d$. The Auger spectrum is given by

$$R_{\mathbf{x}}(\omega) = R_{\mathbf{x}}^0(\omega) \left| \frac{\epsilon_d + \epsilon_{\mathbf{x}} - \omega}{\epsilon_a - \omega} \right|^{2\rho U'}, \quad (13)$$

which has a divergence since $U' < 0$. $R_{\mathbf{x}}(\omega)$ is displayed in Fig. 2 which shows the Auger spectrum on a binding-energy scale. There is a main Auger peak which moves with photon energy on this scale since the Auger line is actually at constant kinetic energy, not constant binding energy. In addition, there is a satellite line at constant binding energy. Near the photon threshold energy

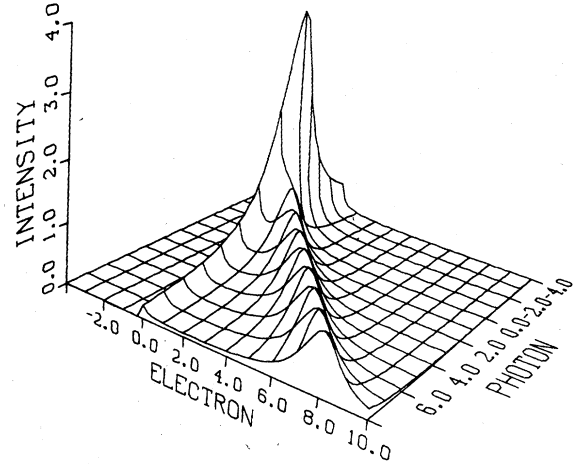


FIG. 2. Calculated Auger spectrum for the case $U = 0$, $U' \neq 0$. Auger intensity is plotted on the z axis, electron binding energy on the x axis, and photon energy on the y axis. The diagonal ridge is the usual Auger spectrum. The ridge at zero binding energy is the satellite peak. The two merge at threshold (photon energy equal to zero). The figure is in units of the core-hole lifetime Γ and is for the case $\rho U' = 0.3$ and a d -hole lifetime of 0.1.

these are indistinguishable and combine to form a large resonant peak in the spectrum. This analytic result is in complete qualitative agreement with the numerical results of DF.

Another limiting case, $U = U'$, may be solved in a similar manner except that scattering events both before and after the Auger decay are included. The result is

$$R_{\mathbf{x}}(\omega) = R_{\mathbf{x}}^0(\omega) \left| \frac{\epsilon_d + \epsilon_{\mathbf{x}} - \omega}{\Lambda} \right|^{2\rho U}. \quad (14)$$

This gives an even stronger satellite relative to the Auger peak since, as DF note, the x-ray-absorption cross section is enhanced at threshold. The two model cases we have investigated, $U = 0$, $U' < 0$, and $U = U'$ span the range of physically reasonable possibilities since for a real system we expect $U \sim U'/2$.

The calculations presented here are not intended to be compared quantitatively with experiment since, as in all analytic calculations of x-ray edge effects, the usual infinite band width (long-time) approximation⁹ has been made. However, these analytic results clearly illustrate the origin of the satellite discovered in the numerical work of DF and show specifically how the present problem is a generalization of the x-ray edge problem.

Consideration of less singular contributions to the Auger rate show that, as in the x-ray edge problem, the exact singularity exponent is the scattering phase shift $2\delta/\pi$ rather than $-2\rho U'$ which is the Born approximation to that quantity.

There is an additional set of less singular terms analogous to the closed loops of the x-ray problem which produce a $-(\delta/\pi)^2$ correction to the exponent. These are rather fine points, however, since the asymptotic region in which the theory is rigorously valid is unlikely to be accessible experimentally.

We close by noting that in addition to further experimental investigations of photoemission

satellites in filled d -shell materials, it would be of great interest to look for this phenomenon in photo- (and electron -impact) induced core-core-core Auger spectra near threshold.

The authors are grateful to J. Houston for assistance with the graphics and to J. W. Gadzuk for useful discussions.

¹T. McMullen and B. Bergersen, *Can. J. Phys.* **50**, 1002 (1972).

²John T. Yue and S. Doniach, *Phys. Rev. B* **8**, 4578 (1973).

³C. O. Almbladh, *Nuovo Cimento B* **23**, 75 (1974).

⁴G. D. Mahan, *Phys. Rev. B* **15**, 4587 (1977).

⁵C. O. Almbladh, *Solid State Commun.* **22**, 339 (1977).

⁶John C. Fuggle, Rainer Lässer, Olle Gunnarson, and Kurt Schönhammer, *Phys. Rev. Lett.* **44**, 1090 (1980).

⁷L. C. Davis and L. A. Feldkamp, *Phys. Rev. Lett.* **44**, 673 (1980).

⁸G. D. Mahan, *Phys. Rev.* **163**, 612 (1967).

⁹P. Nozières and C. T. De Dominicis, *Phys. Rev.* **178**, 1097 (1969).

¹⁰G. D. Mahan, *Solid State Phys.* **29**, 75 (1974).

¹¹M. Cini, *Solid State Commun.* **29**, 605 (1976); **24**, 681

(1977).

¹²M. Cini, *Phys. Rev. B* **17**, 2788 (1978).

¹³G. A. Sawatzky, *Phys. Rev. Lett.* **39**, 504 (1977).

¹⁴G. A. Sawatzky, *Phys. Rev. B* **21**, 1790 (1980).

¹⁵C. J. Powell, *Solid State Commun.* **26**, 557 (1978).

¹⁶M. Iwan, F. J. Himpsel, and D. E. Eastman, *Phys. Rev. Lett.* **43**, 1829 (1979); T. C. Chiang and D. E. Eastman, *Phys. Rev.* **21**, 5749 (1980); M. Iwan and E. E. Koch (unpublished); M. Iwan, E. E. Koch, T. C. Chiang, D. E. Eastman, and F. J. Himpsel (unpublished).

¹⁷S. Hüfner and G. K. Wertheim, *Phys. Lett.* **47A**, 349 (1974).

¹⁸C. Guillot, Y. Ballu, J. Paigné, J. Lecante, K. P. Jain, P. Thiry, R. Pinchaux, Y. Pétroff, and L. M. Falicov, *Phys. Rev. Lett.* **39**, 1632 (1977).

¹⁹David R. Penn, *Phys. Rev. Lett.* **42**, 921 (1979).